Mammalian mitochondrial complex I structure and disease-causing mutations.

Karol Fiedorczuk[1,2] and Leonid A. Sazanov[1,*]

[1]*Institute of Science and Technology Austria, Am Campus 1, Klosterneuburg 3400, Austria.*

[2]*Present address: The Rockefeller University, 1230 York Avenue, New York, NY 10065, USA*

Correspondence: sazanov@ist.ac.at (L. Sazanov)

Abstract

Complex I has an essential role in ATP production by coupling electron transfer from NADH to quinone with translocation of protons across the inner mitochondrial membrane. Isolated complex I deficiency is a frequent cause of mitochondrial inherited diseases. Complex I has also been implicated in cancer, ageing and neurodegenerative conditions. Until recently, the understanding of complex I deficiency on the molecular level was limited due to the lack of high-resolution structures of the enzyme. However, due to developments in single particle cryo-electron microscopy, recent studies have reported nearly atomic resolution maps and models of mitochondrial complex I. These structures significantly add to our understanding of complex I mechanism and assembly. The disease-causing mutations are discussed herein their structural context.

Mitochondrial Disease and Complex I Deficiency

The mitochondrial respiratory chain is responsible for converting energy produced during metabolism into ATP. Electrons harvested from the catabolic processes in the form of NADH enter the chain *via* the proton-pumping NADH-ubiquinone oxidoreductase (complex I or CI), the largest and the most elaborate component of the chain. These electrons are then passed via ubiquinone (hydrophobic electron carrier) to the proton-pumping ubiquinone-cytochrome c oxidoreductase (complex III, existing as a functional dimer $CIII_2$) and, finally via cytochrome c to the proton-pumping

cytochrome c oxidase (complex IV or CIV), which catalyzes the reduction of molecular oxygen to water [1]. These complexes transport protons out of the mitochondrial matrix, generating the electrochemical proton gradient across the inner membrane, used by ATP synthase (complex V) to synthesize ATP [2]. About 30% of mitochondrial diseases affecting energy metabolism can be traced to mutations in the nuclear or mitochondrial DNA encoding the subunits of mitochondrial complex I [3]. On the molecular level, all of the diseases are characterized by defects in oxidative phosphorylation, but patients' symptoms vary widely in nature and severity. Unfortunately, general prognoses are poor. About 50% of patients diagnosed with complex I deficiency die within the first two years of life and only 25% reach the age of ten [4]. The first signs are usually observed shortly after birth and affect the central nervous system. The most common clinical presentations are Leber's hereditary optic neuropathy (LHON), infantile-onset Leigh syndrome, fatal neonatal lactic acidosis, childhood-onset mitochondrial encephalomyopathy and lactic acidosis and stroke-like episodes syndrome (MELAS) [5] (Table 1).

A general genotype-phenotype correlation has not been clearly established so far [6]. It is not well understood how mutations in certain complex I related genes translate to specific clinical phenotypes. An often-cited example of this ambiguity is a mutation in position Arg340 of the ND4 subunit. Substitution to histidine causes LHON syndrome [7] but that to serine results in Leigh syndrome [8] (Table 1).

Additionally, prediction of clinical features based on sequencing data is limited due to the fact that patients are often heterozygotes or display various levels of mitochondrial heteroplasmy in different tissues [9] [10]. Thus, clinical representation of complex I deficiency is an outcome of translation from a number of different 'natural' variants and corrupted gene alleles. Resulting haploinsufficiency can lead to improper complex I assembly or insufficient respiration levels (Table 1). Furthermore, there are at least 15 assembly factors known to be required for the complete maturation of complex I [11,12]. Mutations in most of them can also cause complex I deficiency and associated mitochondrial disease [11].

A better understanding of complex I dysfunction caused by mutations has been obstructed by the lack of high-resolution models for mitochondrial complex I. Until

recently most of the data regarding the atomic structure of the complex was obtained from X-ray crystallography models of bacterial enzymes [13-15]. In general, bacterial complex I consists of 14 "core" protein subunits found in two main domains: seven hydrophilic subunits form the peripheral arm (or matrix arm in mitochondrial enzyme) and seven hydrophobic subunits form the membrane arm. In each catalytic cycle, the transfer of two electrons from NADH to ubiquinone (Q) is tightly coupled to the translocation of four protons across the membrane [16]. These processes are spatially separated. Electron transfer takes place in the matrix arm, which contains all the redox cofactors, including primary electron acceptor FMN, connected via seven FeS clusters to the Q binding site at the interface with the membrane arm (Figure 1 and Box 1). The energy released in this redox reaction drives proton translocation in the membrane arm, containing four putative proton channels [15]. The core is highly conserved from bacteria to humans and forms a functional foundation of the more elaborate, containing many additional subunits, mitochondrial enzyme (Figure 1) [17,18]. Bacterial structures thus provide a good model to understand the general principles of complex I function; however, the role of 31 accessory or "supernumerary" subunits in the mitochondrial enzyme, increasing its total molecular weight from ~ 550 to ~ 980 kDa, remained enigmatic. In eukaryotes, all seven hydrophobic core subunits of complex I are encoded in the mitochondrial DNA (NDx subunits), while seven hydrophilic core subunits and all supernumerary subunits are nuclear-encoded (NDUFx subunits). A first crystal structure of the mitochondrial enzyme was determined at 3.8 Å resolution using enzyme from aerobic yeast *Yarrowia lipolytica*, providing partial atomic models of core subunits while supernumerary subunits were mostly unidentified and modelled as poly-alanine [19]. In 2016, thanks to developments in cryo-electron microscopy (cryo-EM) technology, several models of mammalian complex I from different species were published [20-23].

Here we will compare these structures and discuss briefly how they add to our understanding of complex I mechanism and function. We then review disease-causing single amino acid substitutions in the enzyme. Throughout the review, we will use human nomenclature for the complex I subunits with bovine names in parentheses. Residue numbers are according to sequence numbers of the open reading frame of the gene (i.e. including mitochondrial targeting sequence) as is traditional in the medical

literature, although Table 1 also includes residue numbers in the mature (mitochondria-targeting sequence cleaved) nuclear-encoded subunits as present in the structures.

Comparison of recently published models.

In 2016, a partial model (65% atomic for core subunits and 27% atomic for supernumerary subunits) for bovine [20] and nearly complete (88% atomic) ovine [21] and (84% atomic) porcine [22] models of mitochondrial complex I became available at 4.3Å, 3.9Å and 3.6Å resolution respectively. The subunit composition of these enzymes is identical to human, with about 85% average sequence identity [24], therefore they represent very good models for human complex I as well. In mammalian mitochondria the respiratory chain is organized mostly into supercomplexes or "respirasomes" and CI exists mainly as part of a larger assembly along with $CIII_2$ and CIV [25,26]. The porcine CI structure was solved using supercomplex $CI+CIII_2+CIV$ and unfortunately, suffers from several flaws. Although maps from focused refinement of the matrix and membrane arms individually are of good quality, the map of the entire complex is blurry around the matrix arm. Most EM maps describing the intermediate states of processing are of the wrong hand (mirror image) in all three supercomplex publications from this group [22,23,27]. This can happen with the first dataset if the de novo starting model is generated and used until the hand is flipped in the final rounds of processing. However, why this happened again in two subsequent studies, when the starting supercomplex model should have been available, is not clear. Furthermore, the porcine complex I structure is described as being completely novel, even though the paper [22] was submitted nearly a month after the ovine structure was published [21]. In the deposited porcine model (PDB 5GUP) the B-factors are not refined, the iron-sulphur cluster geometry and environment are incorrect (e.g. 4Fe-4S clusters are ideal cubes instead of known distorted cubane shape with non-planar rhombic faces and T_d symmetry, while Fe atoms are not linked to coordinating residues), the flavin mononucleotide (FMN) isoalloxazine ring is flipped, the non-existing (cleaved) mitochondrial targeting sequence of 24 kDa subunit is built into 10 kDa subunit density, sequence assignment to density in some areas is wrong and model statistics were not reported, among other problems. More recently, the structure of the human respiratory supercomplex, including complex I, was published by the same group [23]. Again, even

though the focused maps are of good quality, the work suffers from the similar problems as listed above. Also, in some areas the ovine complex I model is more consistent with the experimental cryo-EM density for human protein than the deposited human model. Therefore we use the ovine model (as it is higher resolution and more complete than the bovine model, except for the NDUFA11/B14.7 subunit, which is better resolved in the bovine study) as a reference model here. It was used as a basis for the homology model of the human enzyme, which was built in SWISSMODEL [28] using PDB 5LNK, followed by energy minimization in PHENIX [29].

As expected from the sequence comparisons [24] all the models are very similar on the level of tertiary structure. However, on the level of quaternary structure, changes in the position of the peripheral arm (PA) relative to the membrane domain (MD) can be observed (Figure 2). It is also evident that previously discussed modules of the enzyme [18]: N-module (NADH-oxidising part of the peripheral arm, formed around subunits NDUFS1, NDUFV1 and NDUFV2), Q-module (the rest of the peripheral arm, connecting N-module with MD and containing most of the quinone-binding site) and the distal (Pd, formed around subunits ND4 and ND5) or proximal (Pp, the rest of MD) parts of the membrane domain (Figure 1) can move roughly as individual rigid bodies.

Interestingly, comparison of models reveals a link between the positions of the PA relative to the MD and conformation of the catalytically important $\beta1$-$\beta2^{\text{NDUFS2(49kDa)}}$ loop (Figure 2F). The bovine and porcine models have both arms closer (the angle between the arms is smaller) and their PAs are rotationally closer to each other than the ovine model (Figure 2A-E). This position correlates with the $\beta1$-$\beta2^{\text{NDUFS2(49kDa)}}$ loop being retracted from the cavity, which would allow for Q reduction. In the ovine model, the PA and MD are more distant from each other and the loop is inserted, blocking the Q site (Figure 2F, blue). This change is accompanied by a different arrangement of the nearby $\alpha5$-$\alpha6^{\text{ND1}}$ loop and the $\alpha1$-$\alpha2^{\text{ND3}}$ loop, known to be crucial [30] for the active/de-active (A/D) transition first observed many years ago [31].

It is possible that these different quaternary structures correspond to the A/D conformations [32-34] or to different catalytic states of the molecule, hinting at possible intermediates in the putative conformational coupling mechanism proposed by us (Box 1). This is essentially a "one-stroke" per catalytic cycle model. Alternative proposals

include a "two-strokes" model whereby two events of stabilisation of anionic ubisemiquinone and ubiquinol are coupled to two sets of conformational changes each leading to translocation of two protons, resulting in four protons per cycle [19]. Another proposal is the electrostatically driven "wave-spring" model, whereby the cascade of electrostatic interactions spreads along the membrane domain of complex I, leading to alternating protonation and deprotonation of key lysines in antiporter-like subunits, resulting in proton translocation across the membrane [35]. The exact nature of the mechanism remains the hot topic for future investigations.

Complex I deficiency-causing mutations.

In patients suffering from complex I deficiency, mutations have been found in all of the core subunits and in most of the accessory subunits [36]. Changes in the sequence of the core subunits may alter the catalytic mechanism of the enzyme. Accessory subunits are not regarded to be directly involved in catalysis but it has been shown that most of them are indispensable for complex I maturation [37]. This is why mutations in the supernumerary subunits are more likely to cause complex disassembly.

In addition maturation of complex I is also heavily dependent on different assembly factors. They are mostly associated with defined structural modules of the enzyme, such as N-, Q-, Pd and Pp-modules, and mutations in or deletions of these factors cause accumulation of corresponding sub-complexes [11]. Some of the assembly factors are homologous to structural subunits of complex I and serve as their "place holders" in assembly intermediates (e.g. NDUFAF2, a homologue of the NDUFA12 subunit [37]), while others are involved in post-translational modifications (e.g. NDUFAF5, an arginine hydroxylase of Arg73 in NDUFS7 [38], or NDUFAF7, required for dimethylation of Arg85 in NDUFS2 [39]). Factors helping in the folding of MD subunits often contain TM helices themselves (e.g. TIMMDC1, TMEM126B, TMEM70 [40]). Therefore, it is not surprising that many known mutations in assembly factors are associated with human disease [11,12].

In general, human diseases are caused by a wide range of often heterozygous mutations in nuclear DNA or by displaying various levels of mitochondrial heteroplasmy in

different tissues. The mutations can involve either structural subunits of complex I or its assembly factors, and include substitutions, insertions, deletions, inversions, duplications etc. leading to no or pre-maturely terminated protein translation. In this review, we will focus only on single amino acid mutations in structural subunits of complex I identified in complex I deficiency patients (Table 1). Information about disease-causing substitutions and corresponding phenotypes was acquired from HGDM, ClinVar and Mitomap databases. Results of extensive modelling by many research groups of some of these mutations, involving core subunits, in bacteria or lower eukaryotes, were summarised in our previous publications [14,15,41] and reviewed by others [35,42-45].

Interestingly, most of the LHON-linked mutations map to the membrane domain, while Leigh syndrome and other diseases are mostly caused by mutations in the peripheral arm (Figure 3). This could be related to a potential link between defects in the proton pumping apparatus and LHON-like phenotype.

Core Subunits of the Peripheral (Matrix) Arm

NDUFS1 (75kDa) subunit
The reported mutations Val71Asp, Gly166Glu, Val228Ala, Leu231Val, Arg241Trp are located in close proximity to Fe-S clusters (Figure 4A). They form part of the loops crucial for the proper binding and stability of the clusters. For example, Val71 is located in the proximity of the N3 and N1b clusters in a loop interacting directly with cluster-coordinating side chains.
Other mutations Asp252Gly, Arg408Cys, Gln522Lys, Thr595Ala, Asp619Asn, Tyr695His/Cys and Met707Val are located in regions important for complex assembly (Table 1).

NDUFV1 (51kDa) subunit
The NDUFV1 subunit coordinates FMN, the primary electron acceptor [13]. Many mutations are located around the FMN binding site where NADH is oxidized and electron transfer starts Arg88Gly, Tyr204Cys, Cys206Gly, Ala211Val. Others, Pro122Leu, Glu214Lys, Arg386Cys, Thr423Met, Ala422Pro affect Fe-S cluster

binding, while Ser56Pro, Lys111Glu, Arg147Trp, Arg199Pro, Ala341Val are likely to affect the stability of the whole NADH oxidizing module (Figure 4B). Mutations that are not placed close to the catalytically important centres of the subunit and are more likely to affect assembly or perhaps FMN binding and Fe-S cluster stability in a more indirect way are Ser56Pro, Arg199Pro, Pro252Arg and Ala341Val.

NDUFS2 (49kDa) subunit

The Arg118Gln, Arg138Gln, Ala224Val mutations are located around the terminal N2 cluster and can influence both the reduction of the cluster and electron transfer from N2 to ubiquinone. In mammalian complex I, Arg118 undergoes an unusual dimethylation [39]. The guanidino group of the side chain is in direct contact with cluster N2. It has been proposed that it contributes to the relatively high reduction potential of the cluster [13,46]. Mutation in this position will likely impact the redox potential of the cluster. Arg138 similar to Arg118 is placed very close to N2 with one nitrogen of the side chain only 2.8Å away from the nearest sulphur of the cluster and its mutations have a dramatic effect on the properties of this redox center [47]. Mutation to Gln will likely lower the N2 redox potential and affect electron transfer rates. Although Ala224 does not influence the N2 cluster directly, it is placed next to His223, which was proposed to be the redox-Bohr group associated with the cluster [48] and like the arginines, defines the environment for the N2 cluster (Figure 4C).

Other mutations of the NDUFS2 subunit (Asp110Val, Glu148Lys, Arg228Gln, Pro229Gln, Met292Thr, Arg323Gln, Arg333Gln, Ser413Pro, Met443Lys) are localized in regions important for the subunit's stability or interactions with other subunits (Table 1).

NDUFS8 (TYKY) subunit

The N-terminal end of the NDUFS8 subunit is composed of two connected amphipathic α-helices located on the matrix side of the internal mitochondrial membrane. One possible role of these α-helices is to stabilize the position of the PA relative to the lipid bilayer [21]. Thus, they may be important for the regulation of the proposed wedge/rotation like movements of the PA [20,21]. The relevance of these α-helices can also be demonstrated by the analysis of disease-causing substitutions. Arg54Trp, Glu63Gln, Arg77Trp and Pro79Leu are all located either on or in close proximity to

these helices. Additionally, this region of NDUFS8 is in contact with the NDUFA13 (B16.6), ND1, NDUFA3 (B9), NDUFA7 (B14.5a) subunits and a cardiolipin molecule.

Other mutations, Arg102His, Arg138His, Gly154Ser, Ala159Asp likely cause destabilization of Fe-S clusters. Arg102 and Arg138 are found on coils in direct contact with loops binding cluster N5. Ala159 is placed right next to Cys160 responsible for coordination of cluster N6a (Figure 4D). Pro85Leu and Arg94Cys mutations probably cause misassembly of the subunits (Table 1).

NDUFS7 (PSST) subunit

Val122Met and Arg145His are found on two parallel β-strands that are followed by loops coordinating the terminal N2 cluster. This four-strand β-sheet makes up a great part of the NDUFS7 subunit and is central for the stability of this region at the base of PA (Table 1).

NDUFS3 (30kDa) and NDUFV2 (24kDa) subunits

The NDUFS3 and NDUFV2 subunits are the only core subunits of the peripheral arm that do not take part directly in the main electron transfer path, but rather provide the platform required for complex assembly [49]. Identified disease-causing mutations Thr145Ile, Arg199Trp and Pro223Leu of the NDUFS3 subunit are located mostly at the interfaces with other subunits (Table 1).

The single Lys209Arg substitution in the NDUFV2 subunit is localized at the very periphery of the PA and its role is not clear.

Core Subunits of the Membrane Domain

ND1 subunit

Mutations in this subunit cause a broad spectrum of clinical features, including Alzheimer and Parkinson Disease, MELAS or Leigh syndrome (Table 1). Interestingly, the Ala52Thr mutation is one of the most frequently encountered mutations in LHON syndrome, identified in approximately 13% of cases (together with Arg340His[ND4] [69%] and Met64Val[ND6] [14%] they cause almost 95% of all cases). The broad variety of the diseases caused by substitutions in the ND1 region can be explained by the subunit's involvement in several different functions. It contains the quinone binding

chamber, creates the proton input channel for the first translocation channel (the so-called E-channel) and directly enables coupling as it links the Q-chamber with proton pumping modules (Box 1). Disease-causing mutations can affect all of those functions. Those that probably impact the accessibility to quinone are Val11Met, Glu24Lys, Leu28Met, Tyr30His, Met31Val, Ala52Thr, Met53Ile, Glu59Lys and Tyr227Cys. The conformational coupling between the Q site and the proton pumps may be affected by Val208Leu, Arg195Gln, Glu214Lys and Tyr215His. Mutations Ser110Asn, Ala112Thr, Glu143Lys, Gly131Ser and Ala132Thr are most likely to affect proton pumping activity of the E-channel. Additionally, substitutions Thr164Ala, Thr240Met, Leu285Pro and Leu289Met probably cause the enzyme's dysfunction by affecting its structural stability (Figure 4E, Table 1).

ND6 subunit

Mutations in the ND6 subunit can be classified into three groups, those likely to affect proton translocation directly: Gly36Ser, Tyr59Cys, Met63Val, Met64Ile, Met64Val and Leu60Ser (Figure 4F); those affecting proton translocation indirectly: Ile26Met, Ala72Val and Ala74Val; and those likely to have an effect on complex I structural stability: Asn117Asp and Ser132Leu (Table 1). All the mutations from the first group are located very close to the π-bulge (disrupted secondary structure rendering α-helix flexible) on the highly conserved TM3, thought to be crucial for conformational coupling in complex I [15].

ND3 subunit

Most of the mutations in the ND3 subunit: Ser34Pro, Ser45Pro, Ala47Thr, Ile60Thr and Glu66Asn are found in the putative catalytically important regions. Ser34, Ser45 and Ala47 are all located on the long loop of ND3 that traverses the membrane domain on the matrix site of the mitochondria. Although none of these amino acids are conserved [14] they may affect the catalytic turnover of complex I indirectly, since the loop plays a key role in the A/D transition of the enzyme [50] and stabilises the peripheral arm / membrane arm interface (Box 1).

Glu66 is on a TM helix next to highly conserved key TMH3^{ND6} and so any disturbance in this area may restrict/change conformational space available to TMH3^{ND6} [21] (Table 1).

ND4L subunit

Val65Ala and Cys32Arg are both located close to the sites crucial for proton pumping [21]. Val65 is situated next to the protuberance (π-bulge) of the TMH3^{ND6} very close to the key residues of ND4L and ND6. Cys32 is located next to the key Glu34 and Tyr69^{ND6} [21] (Table 1).

ND2 and ND4 subunit

All the known mutations of the ND2 subunit: Ile57Met, Leu71Pro, Gly259Ser and the ND4 subunit: Ile165Thr, Val313Ile, Arg340Ser, Arg340His, Tyr409His are localized in regions likely important for complex I stability, not catalysis. One exception is Arg340^{ND4} which interacts with the negatively charged C-terminus of the key TM7^{ND4}, so the mutation may impede catalytically relevant movements of this key discontinuous helix (Table 1).

ND5 subunit

Mutations Phe124Leu, Glu145Gly, Ala171Val, Ala236Thr, Met237Leu, Ser250, Asp393Asn/Gly and Gly465Glu most likely affect the catalytic function of the ND5 subunit. Phe145, Ala171, Ala236, Met237 build the entry channel for the protons; Phe124 and Ser250 influence connections of the input and output channels; while Asp393 and Gly465 are involved in the architecture of the output pathway. Other substitutions, Tyr159His and Gln434Arg probably play a more structural role (Figure 4I, Table 1).

Supernumerary Subunits Associated with the Peripheral (Matrix) Arm

NDUFS6 (13kDa) subunit

Cys115Tyr substitution is the only known single amino acid disease-causing mutation for this subunit and it has been previously discussed in the ovine complex I study [21]. Conserved Cys115 is one of the residues coordinating the zinc ion bound to this subunit (Box 1, Figure 4G). Mutation of Cys115 to another amino acid not only would destabilize the zinc-binding site, but it may also decrease electron transfer efficiency by disturbing the N5 cluster and perhaps affect regulatory capabilities of the system [21,51].

NDUFA9 (39kDa) subunit

The reported mutation Arg321Pro concerns one of the amino acids coordinating the NADPH molecule buried in the centre of the NDUFA9 subunit (Figure 4J). Mutation likely causes loss of the co-factor and distortion of the whole subunit [52], which results in decreased complex I activity [53]. It has been also proposed that precise positioning of the NADPH co-factor can indirectly regulate the function of the terminal N2 cluster [21]. Another mutation Arg360Cys is located on a loop forming contacts with other subunits.

NDUFS4 (18kDa) subunit

The disease-causing mutation Asp119His is proposed to affect the stability of the complex. This residue is not likely to play a catalytic role but it has been shown that subunit NDUFS4 is important for the assembly of the complex [37] (Table 1).

Supernumerary Subunits Associated with the Membrane Domain

NDUFA10 (42kDa) and NDUFB9 (B22) subunits

These subunits are located on the matrix side of the membrane domain. The disease-causing mutation Gly99Glu^{NDUFA10} is located at the interface with the ND2 and NDUFC1 (KFYI) subunits, so it may decrease the stability of the complex in this region. The Gln142Arg^{NDUFA10} mutation is found in the central α-helix of the subunit, within the nucleotide kinase fold and most likely affects the structure (Figure 4L).

One mutation of NDUFB9 is reported to cause complex I deficiency (Table 1) and it is likely to influence subunit assembly. This mutation (Leu64Pro) occurs at the last α-helix of the NDUFB9 helical bundle accommodating the phosphopantetheine (PNS) co-factor covalently bound to the NDUFB9's interacting partner NDUFAB1-β (SDAP-β) subunit (Box 1). A mutation to proline in the middle of the helix can affect the structure of the PNS hydrophobic pocket and alter the NDUFAB1/NDUFB9 complex causing destabilization of this region (Figure 4H).

NDUFA1 (MWFE), NDUFA8 (PGIV) and NDUFA13 (B16.6) subunits

These subunits are located mostly on the IMS site of the membrane domain. They mostly play stabilizing roles, important for enzyme assembly [37]. Reported disease-

causing mutations Gly8Arg, Gly32Arg, Arg37Ser, Tyr43His of NDUFA1 and Lys5Asn of NDUFA13 are mainly located on the interfaces with other complex I subunits (Figure 4K, Table 1). The reported mutation 325G>A in the NDUFA8 gene results in Glu109Lys substitution. However, in position 109 Lys is a natural variant in some mammals (e.g. Ovis Aries) [24]. It is likely that the mutation does not strongly affect the protein but causes instability of the NDUFA8 gene transcript [54].

Concluding Remarks and Future Perspectives.

There is no cure for complex I related diseases. The current best treatment is to optimize nutrition and reduce physiological stress. Pharmacological treatment includes supplementation with CoQ, riboflavin, L-creatine, L-arginine, L-carnitine and vitamins: B1, C, E and folinic acid (reduced form of folic acid) [55]. The recent structures of mitochondrial complex I have already provided a great insight into its mechanism and function. They improved not only our understanding of the very basic processes in our cells – ATP production - but can also become a starting point for structure-based, in-silico design of the new type of molecules for a better treatment of patients suffering from complex I deficiency [56].

Recent progress was accomplished thanks to the latest developments in cryo-EM [57]. Currently, only single particle cryo-EM allows achievement of resolutions high enough to obtain maps of mammalian complex I interpretable on the atomic scale. One of the main remaining questions in the field is the exact nature of the enzyme's coupling mechanism (see "Outstanding Questions"). It can be studied by determining the structures of complex I in different redox states and in the presence of various substrates/inhibitors, visualizing conformational changes underlying coupling mechanism. Another question is on the role of respiratory supercomplexes, a dominant physiological state of the electron transport chain [25]. It is not yet clear if they provide any kinetic advantage for the respiratory reactions or mainly stabilize individual complexes or perhaps limit ROS production [26]. Atomic structures of the supercomplexes (CI+CIII$_2$, CI+CIII$_2$+CIV, CIII$_2$+CIV$_n$, etc) are being determined [22,23], however, inter-complex contacts at the side-chain level are not yet established due to limited resolution in the reconstructions of the entire assemblies. This precludes

the detailed analysis of the role of individual residues in such contacts. Cryo-electron tomography already allows us to look at the respiratory chain enzymes (supercomplexes) in the native lipid environment, albeit at low resolution so far [58,59]. This will continue to improve and will provide complementary information to the structures coming from single particle analysis. Further developments in cryo-EM technology will undoubtedly continue to provide us with exciting new knowledge on the organisation of the respiratory chain.

Table 1. Summary of single amino acid substitutions causing complex I deficiency.

Subunit name Human/ Bovine	Location	Mutation (residue # in nuclear-encoded mature subunit)	Remaining activity of complex I (%)	Additional comments	Reported clinical feature	Proposed reason for complex I dysfunction	Reference
NDUFS1 / 75kDa	Peripheral domain/ core	Val71Asp (48)	<50		Miscellaneous: raised blood lactate, raised CSF lactate, muscular hypotonia, psychomotor development delay	Disruption of electron transfer at N1b and N3 clusters site; located close to the clusters in a loop interacting with cluster-coordinating chains.	[60]
		Gly166Glu (143)	<50		Miscellaneous: optic atrophy, psychomotor regression, nystagmus, dystonia and dysphagia, leukodystrophy, brain atrophy, symmetrical lesions affecting pons and medulla oblongata	Disruption of electron transfer at N1b cluster site; located close to the cluster, part of a loop followed by a β-sheet and a coil that binds N1b cluster	[61]
		Val228Ala (205)	>50	Accumulation of subcomplexes	Leukoencephalomyelopathy	Disruption of electron transfer at N1b and N3 clusters site; located in a loop between the N3 and N1b clusters 5.4 Å and 3.9 Å away respectively	[62-64]
		Leu231Val (208)	25		Leigh syndrome	Disruption of electron transfer at N4 cluster site	[65]
		Arg241Trp (218)	77	Oxidation of NADH-generating substrates was low in muscle mitochondria, in fibroblasts, and in circulating lymphocytes	Miscellaneous: growth retardation, axial hypotonia, hepatomegaly, persistent hyperlactatemia, hyperintensity of basal ganglia, macrocytic anemia and dystonia	Disruption of electron transfer at N5 and N6 clusters site; side chain ~3Å away from cysteines coordinating these clusters	[66]
		Asp252Gly (229)	67	A complex I deficiency was identified in muscle and liver. Decreased NADH-generating substrates oxidation in fibroblasts suggested a complex I deficiency. Lymphocytes were normal	Leukoencephalomyelopathy	Affected assembly due to misfolding of NDUFS1 subunit; located in region central for proper folding of the subunit	[62,66]
		Arg408Cys (385)	<30	Accumulation of subcomplexes	Leukoencephalomyelopathy	Affected assembly due to misfolding of NDUFS1 subunit; located in region central for proper folding of the subunit	[64]
		Gln522Lys (499)	45	Formation of ~800 kDa subcomplex ; increased level of ROS production , affinity for NADH	Leukoencephalomyelopathy	Affected assembly due to misfolding of NDUFS1 subunit; located in region central for proper folding of the subunit	[54]
		Thr595Ala (572)	<50		Leukoencephalomyelopathy	Affected assembly due to misfolding of NDUFS1 subunit	[67]
		Asp619Asn (596)	<30	Accumulation of subcomplexes	Isolated enzymatic complex I deficiency confirmed in both muscle tissue and cultured fibroblasts	Affected assembly due to impaired interaction of NDUFS1 and NDUFA6 (B14) subunits; in a loop close to the NDUFS1/NDUFA6 interface	[64,68]
		Tyr695His (672)	<50		Miscellaneous: raised blood lactate, leukodystrophy, lactate raised in brain, loss of neurological abilities	Affected assembly due to misfolding of NDUFS1 subunit; close to Met707	[60,63]
		Tyr695Cys (672)	<50		Miscellaneous: raised blood lactate, leukodystrophy, lactate raised in brain, loss of neurological abilities	Affected assembly due to misfolding of NDUFS1 subunit; close to Met707	[60]
		Met707Val (684)	50	A complex I deficiency was identified in muscle. Cultured skin fibroblasts oxidized NADH-generating substrates normally	Miscellaneous: hypotonia, microcephalia, and pyramidal syndrome, Leigh syndrome, and permanent anemia	Affected assembly due to misfolding of NDUFS1 subunit; close to Tyr695	[66]
NDUFV1/ 51kDa	Peripheral domain/ core	Ser56Pro (36)	<50		Miscellaneous: brain abnormalities, motor delay including pyramidal signs, hypotonia and a mild ataxia, minor cognitive impairment	Affected assembly due to impaired interaction of NDUFV1, NDUFV3 (10kDa) and NDUFV2 subunits, located at α-helix that makes interactions with the NDUFV3 and C-terminal extension of NDUFV2 subunit	[4]

		Arg88Gly (68)	N/A	A muscle biopsy was inconclusive, no clear changes of a mitochondrial cytopathy	Leigh syndrome	Disruption of electron transfer at FMN site; builds the pocket for FMN binding	[69]
		Pro122Leu (102)[b]	<20		Miscellaneous: stroke, exercise intolerance, dyspnoea, leukodystrophy	Disruption of electron transfer at FMN and N1a cluster sites; located in a loop between FMN and cluster N1a	[70]
		Arg199Pro (179)	N/A	Arginine was conserved at position 199 in all 46 other vertebrate species analyzed	Leigh syndrome	Affected assembly due to impaired interaction of NDUFV1, NDUFV3 and NDUFV2 subunits; located in a β-strand interacting with the NDUFV3 and NDUFV2 subunits	[69]
		Tyr204Cys (184)	30	A complex I deficiency was identified in muscle. Oxidation of NADH-generating substrates was normal in both cultured skin fibroblasts and circulating lymphocytes	Miscellaneous: ptosis and strabismus, ataxia, bilateral ptosis, ophthalmoplegia, metabolic acidosis, hyperintensity of the locus niger	Disruption of electron transfer at FMN site; builds the pocket for FMN binding	[66]
		Cys206Gly (186)	30	A complex I deficiency was identified in muscle. Oxidation of NADH-generating substrates was normal in both cultured skin fibroblasts and circulating lymphocytes	Miscellaneous: ptosis and strabismus, ataxia, bilateral ptosis, ophthalmoplegia, metabolic acidosis, hyperintensity of the locus niger	Disruption of electron transfer at FMN site; placed close to residues crucial for FMN and NADH binding including Glu189	[66]
		Ala211Val (191)	<55	A complex I deficiency was identified in cultured decidual cells. No deficiency in native chorionic villi nor muscle (aborted fetus)	Miscellaneous: brain abnormalities, motor delay including pyramidal signs, hypotonia and a mild ataxia, minor cognitive impairment	Disruption of electron transfer at FMN and N3 cluster sites; located very close to FMN and N3 coordinating residues	[71]
		Glu214Lys (194)	50	A complex I deficiency was identified in muscle and liver. Oxidation of NADH-generating substrates was normal in cultured skin fibroblasts.	Miscellaneous: acrocyanosis, muscular hypotonia, pendular nystagmus, bitemporal retinal depigmentation, increased latencies of the visual evoked potentials, lactic acidosis	Disruption of electron transfer at FMN and N3 cluster sites and affected assembly due to impaired interaction of NDUFV1 and NDUFS1 subunits; placed in between coils stabilizing FMN and binding cluster N3	[66]
		Ala341Val (321)	<36	Isolated complex I deficiency was detected in muscle, data form cultured fibroblasts inconsistent	Miscellaneous: infantile myoclonic epilepsy, spasticity, macrocephaly, brain atrophy, leukodystrophy, blindness	Disruption of electron transfer at FMN site due to possible distortion of the NADH-binding pocket	[54,72]
		Arg386Cys (366)	<40	Complex I assay (n-decyl CoQ) 0% Complex I assay (CoQ1) 38%	Leukoencephalomyelopathy	Disruption of electron transfer at N3 cluster site and affected assembly due to misfolding of NDUFV1 subunit; located next to the conserved Cys385 coordinating cluster N3	[73]
		Thr423Met (403)	N/A		Broad spectrum	Disruption of electron transfer at N3 cluster site and affected assembly due to misfolding of NDUFV1 subunit; located next to the conserved Cys425 coordinating cluster N3	[72]
		Ala432Pro (412)	50	A complex I deficiency was identified in muscle and liver. Oxidation of NADH-generating substrates was normal in cultured skin fibroblasts.	Miscellaneous: vomiting, hypotonia, lethargy, apnea, metabolic acidosis, hyperintensity in the basal ganglia	Disruption of electron transfer at N3 cluster site due to distortion of the α-helix directly linked to the conserved Cys425 coordinating cluster N3	[66]
NDUFS2 / 49kDa	Peripheral domain/ core	Asp110Val (77)	<25		Cardiomyopathy	Affected assembly due to impaired interaction of NDUFS2, NDUFS3, NDUFS7 and ND1 subunits; located in the middle of a β-strand that is part of a β-sheet interacting with the NDUFS3, NDUFS7 and ND1 subunits	[60]
		Arg118Gln (85)	20	heterozygous mutation in addition to NDUFS2/ Met292Thr	Leigh syndrome	Disruption of electron transfer at N2 cluster site, affects the redox potential of the cluster	[9]
		Arg138Gln (105)	16	heterozygous mutation same patient as NDUFS2/ Arg333Gln	Leigh syndrome	Disruption of electron transfer at N2 cluster site, affects the redox potential of the cluster	[9]

Subunit	Domain	Mutation (position)	Activity (%)	Notes	Disease	Effect on assembly/mechanism	Ref.
		Glu148Lys (115)	13	heterozygous mutation in addition to NDUFS2/ Met292Thr	Leigh syndrome	Affected assembly due to misfolding of NDUFS2 subunit; located at an α-helix in the center of the NDUFS2 subunit	[9]
		Ala224Val (191)	13	complex I activity was markedly low in muscle but was normal in cultured fibroblasts	Miscellaneous: neonatal hypotonia, dysmorphic features, epilepsy and signs of brainstem involvement, lactic acidosis	Disruption of electron transfer at N2 cluster site; placed next to His190, which was proposed to be the redox-Bohr group associated with the cluster	[54]
		Arg228Gln (195)	<60		Cardiomyopathy and encephalomyopathy	Affected assembly due to impaired interaction of NDUFS2 and NDUFS8 subunits; located close to the interface with NDUFS8 subunit	[74]
		Pro229Gln (196)	<36		Cardiomyopathy and encephalomyopathy	Affected assembly due to impaired interaction of NDUFS2 and NDUFS8 subunits; located close to the interface with NDUFS8 subunit	[74]
		Met292Thr (259)	<30		Leigh syndrome	Affected assembly due to impaired interaction of NDUFS2, NDUFS3, NDUFA5 (B13), NDUFC2 (B14.5b) and NDUFS8 subunits	[9,75]
		Arg323Gln (290)	<25		Cardiomyopathy	Affected assembly due to impaired interaction of NDUFS2, NDUFA5 and NDUFS8 subunits	[63]
		Arg333Gln (300)	16	heterozygous mutation same patient as NDUFS2/ Arg138Gln	Leigh syndrome	Affected assembly due to impaired interaction of NDUFS2, NDUFA13, NDUFA7 and NDUFS8 subunits	[9]
		Ser413Pro (380)	<70		Cardiomyopathy and encephalomyopathy	Affected assembly due to misfolding of NDUFS2 subunit and impaired interaction of NDUFS2 and NDUFS3 subunits; on a β-strand interacting with NDUFS3 subunit	[74]
		Met443Lys (410)	27	heterozygous mutation in addition to NDUFS2/ Met292Thr	Leigh syndrome	Affected assembly due to impaired interaction of NDUFS2 and ND1 subunits, located at the interface with ND1 subunit	[9]
		Asp446Asn[c] (413)	26		Miscellaneous: basal ganglia and brainstem lesions, seizures, hypotonia, amaurosis, nystagmus	Affected assembly due to interaction of NDUFS2 and ND1 subunits, located at the interface with ND1 subunit	[76]
NDUFS3 / 30kDa	Peripheral domain/ core	Thr145Ile (109)	50		Leigh syndrome	Affected assembly due to misfolding of NDUFS3 subunit, close to the center of a β-sheet forming most of the NDUFS3 subunit	[77]
		Arg199Trp (163)	50		Leigh syndrome	Affected assembly due to impaired interaction of NDUFS3, NDUFS2 and NDUFS4 subunits; found in a loop that directly contacts the NDUFS2 and NDUFS4 subunits	[77]
		Pro223Leu (187)	14		Encephalomyopathy	Affected assembly due to impaired interaction of NDUFS3, NDUFS2, NDUFS7 and NDUFA6 subunits; found at the end of a loop located in between the NDUFS7, NDUFS2 and NDUFA6 subunits	[62]
NDUFV2/ 24kDa	Peripheral domain/ core	Lys209Arg (177)	N/A		Parkinson disease	Not clear, located at peripheral α-helix of the complex	[78]
NDUFS8 TYKY	Peripheral domain/ core	Arg54Trp (20)	29		Progressive external ophthalmoplegia and Leigh syndrome	Affected assembly due to misfolding of NDUFS8 subunit; located at a stabilizing amphipathic α-helix	[79]
		Glu63Gln (29)	<20		Leigh syndrome	Affected assembly due to misfolding of NDUFS8 subunit; located at a stabilizing amphipathic α-helix	[63]
		Arg77Trp (43)	<55		Cardiomyopathy and encephalomyopathy	Affected assembly due to misfolding of NDUFS8 subunit; located close to a stabilizing amphipathic α-helix	[63]
		Pro79Leu (45)	39	Value for the muscle tissue, complex I deficiency also reported for skin fibroblasts, heart, liver and brain	Leigh syndrome	Affected assembly due to misfolding of NDUFS8 subunit; located close to a stabilizing amphipathic α-helix	[80]

Subunit	Domain	Mutation		Notes	Disease	Structural effect	Ref
					tissues		
		Pro85Leu (51)	<43	WB analysis showed decreased amounts of the NDUFS8 protein and other nuclear-encoded complex I subunits	Leigh syndrome	Affected assembly due to impaired interaction of NDUFS8, NDUFA12 (B17.2) and NDUFS7 subunits; located at the loop interacting with the NDUFA12 and NDUFS7 subunits	[81]
		Arg94Cys (60)	18		Complex I deficiency report based on muscle tissue as well as in cultured fibroblasts	Affected assembly due to impaired interaction of NDUFS8 and NDUFS2 subunits; found in a loop making the interface with the NDUFS2 subunit	[76,82]
		Arg102His (68)	39	Value for the muscle tissue, complex I deficiency also reported for skin fibroblasts, heart, liver and brain tissues	Leigh syndrome	Disruption of electron transfer at N5 cluster site; stabilizes loop coordinating cluster N5	[80]
		Arg138His (104)	<43	WB analysis showed decreased amounts of the NDUFS8 protein and other nuclear-encoded complex I subunits	Leigh syndrome	Disruption of electron transfer at N5 cluster site; stabilizes another loop coordinating cluster N5	[81]
		Ala159Asp (125)	<55		Cardiomyopathy and encephalomyopathy	Disruption of electron transfer at N6a cluster site; placed next to Cys126 coordinating cluster N6a. Mutation will likely decrease redox potential of N6a.	[63]
NDUFS7 PSST	Peripheral domain/ core	Val122Met (84)	<80		Leigh syndrome	Disruption of electron transfer at N2 cluster site and affected assembly due to misfolding of NDUFS7 subunit; located on β-strand followed by a loop approaching the N2 cluster	[83]
		Arg145His (107)	62		Leigh syndrome	Disruption of electron transfer at N2 cluster site and affected assembly due to misfolding of NDUFS7 subunit; located on β-strand followed by a loop coordinating the N2 cluster	[84]
MT-ND6 ND6	Membrane domain/ core	Ile26Met	21		Leber hereditary optic atrophy	Disturbance of catalytically important TMH1-2^{ND3} loop or TMH3^{ND6}	[85]
		Gly36Ser	N/A		Leber hereditary optic atrophy	Disruption of proton translocation through the E-channel, facing π-bulge on a highly conserved TMH3	[85,86]
		Tyr59Cys	N/A		Leber hereditary optic atrophy	Disruption of proton translocation through the E-channel, sits on a π-bulge from a highly conserved TMH3, Tyr proposed to be crucial for proton translocation	[85,86]
		Leu60Ser	N/A		Leber hereditary optic atrophy	Disruption of proton translocation through the E-channel, located on a highly conserved TMH3	[85,87]
		Met63Val	<25	Low complex I activity in muscles, normal in fibroblasts	Leigh syndrome	Disruption of proton translocation through the E-channel, located on a highly conserved TMH3	[54]
		Met64Val	N/A	Increased inhibitor sensitivity	Leber hereditary optic atrophy	Disruption of proton translocation through the E-channel, located on a highly conserved TMH3	[88,89]
		Met64Ile	N/A		Leber hereditary optic atrophy	Disruption of proton translocation through the E-channel, located on a highly conserved TMH3	[60,85,90]
		Ala72Val	5		Miscellaneous: juvenile myopathy, encephalopathy, lactic acidosis, stroke	Disturbance of catalytically important TMH1-2^{ND3} loop or TMH3^{ND6}	[91,92]
		Ala74Val	33		Miscellaneous: Leber hereditary optic atrophy with dystonia, Leigh syndrome	Disturbance of catalytically important TMH1-2^{ND3} loop or TMH3^{ND6}	[93,94]
		Asn117Asp	N/A	The substitution is a candidate LHON mutation, but the available evidence is not definitive	Leber hereditary optic atrophy	Affected assembly due to impaired interaction of ND6, ND5, ND4L and ND2 subunits; located in a loop contacting ND5, ND4L and ND2	[95]

		Mutation		Notes	Disease	Structural effect	Ref
		Ser132Leu	N/A		Leber hereditary optic atrophy	Affected assembly due to impaired interactions of subunits at the "heel" of complex I; located at the interface with several supernumerary subunits	[96]
MT-ND5 ND5	Membrane domain/ core	Phe124Leu	<35	Mutation present at levels of 43% load in skeletal muscle and 30% mutant load in skin fibroblasts	Leigh syndrome	Disruption of proton translocation through the ND5 channel; placed in the middle of TMH4, in contact with the residues at the crucial π-bulge of TMH8	[97]
		Glu145Gly	100	Mutation present at 48% in muscle and 15% in blood	MELAS	Disruption of proton translocation through the ND5 channel; one of the key residues accepting protons from the matrix side	[98]
		Tyr159His	N/A	Located in evolutionary not conserved region	Leber hereditary optic atrophy	Affected assembly due to impaired interaction of ND5 and ND4 subunits; directly interacts with ND4 residues on the matrix site of the membrane	[99]
		Ala171Val	N/A		Leber hereditary optic atrophy	Disruption of proton translocation through the ND5 channel; located close to the cavity making an entry point for protons	[100]
		Ala236Thr	23		MELAS, Leigh syndrome	Disruption of proton translocation through the ND5 channel; located close to the cavity making an entry point for protons	[101]
		Met237Leu	Mild defect	Mutation present at 82% in muscle and 13% in blood	Miscellaneous: Leber hereditary optic atrophy, MELAS, Leigh syndrome	Disruption of proton translocation through the ND5 channel; located close to the cavity making an entry point for protons	[98]
		Ser250Cys	Partial CI deficiency	The mutation was detected in a heteroplasmic state in the lymphocytes of the patient's mother (57%), who had migraine and optic atrophy, and younger sister (41%)	MELAS, Leigh syndrome	Disruption of proton translocation through the ND5 channel; located at the crucial π-bulge of TMH8	[102]
		Asp393Asn	15	Normal activity in fibroblasts, reduced WB signal for NDUFS7 and NDUFB6	MELAS, Leigh syndrome	Disruption of proton translocation through the ND5 channel; placed next to the key Lys392 and builds the proton outlet cavity	[54,103]
		Asp393Gly	39	Normal activity in fibroblasts, reduced WB signal for NDUFS7 and NDUFB6	Leigh syndrome	Disruption of proton translocation through the ND5 channel, placed next to the key Lys392 and builds the proton outlet cavity	[54]
		Gln434Arg	N/A	The substitution is a regarded as a possible risk factor for LHON that could contribute to the clinical manifestation of this disease under certain conditions	Leber hereditary optic atrophy	Affected assembly due to impaired interaction of ND5, NDUFB3 (B12) and NDUFB9 subunits, found on a loop that is in direct contact with NDUFB3 and NDUFB9 subunits	[104]
		Gly465Glu	N/A	Mutation present in approximately 80% of the mtDNA molecules	Leber hereditary optic atrophy	Affected assembly due to misfolding of ND5 subunit; located directly opposite to the loop linking two half helices of TMH12	[105]
MT-ND4L ND4L	Membrane domain/ core	Cys32Arg	N/A		Familial colorectal cancer	Disruption of proton translocation through the E-channel; located next to the key Glu34 and Tyr59[ND6]	[106]
		Val65Ala	Partial CI defect		Leber hereditary optic atrophy	Disruption of proton translocation through the E-channel; situated next to the π-bulge of the TMH3 of ND6, close to the key residues of ND4L and ND6 subunits	[107]
MT-ND4 ND4	Membrane domain/ core	Ile165Thr	N/A		Leber hereditary optic atrophy	Affected assembly due to impaired interaction of ND4 and ND2 subunits; placed at the C-terminal end of an α-helix forming the main interaction site with ND2 subunit	[108]
		Val313Ile	21		Miscellaneous: Leber hereditary optic atrophy, Leber hereditary optic neuropathy with dystonia	Affected assembly due to misfolding of ND4 subunit; found on TMH12 far from the proton translocation site	[85]
		Arg340Ser	<45	Resistance to rotenone in humans	Leigh syndrome	Affected assembly due to misfolding of ND4 subunit; located at a loop in contact with the TMH10-11 loop and NDUFB4 (B15) subunit. Arg340 interacts with the negatively charged C-	[54,109,110]

					terminus of the key TM7[ND4], so the mutation may impede catalytically relevant movements of this discontinuous helix.	
		Arg340His	<25		Leber hereditary optic atrophy	Affected assembly due to misfolding of ND4 subunit, located at a loop in contact with the TMH10-11 loop and NDUFB4 subunit. Arg340 interacts with the negatively charged C-terminus of the key TM7[ND4], so the mutation may impede catalytically relevant movements of this discontinuous helix.	[5,7,111]
		Tyr409His	>100	NADH dehydrogenase and succinate dehydrogenase (SDH) activities increased	Leigh syndrome	Affected assembly due to impaired interaction of ND4 and NDUFB8 subunits	[112]
MT-ND3 ND3	Membrane domain/ core	Ser34Pro	<20		Leigh syndrome	Affected complex I active/deactive state transition, located at a loop crucial for the A/D transition of the enzyme	[54,113]
		Ser45Pro	<25		Leigh syndrome	Affected complex I active/deactive state transition, located at a loop crucial for the A/D transition of the enzyme	[54,113]
		Ala47Thr	12	Activity from muscle homogenate. Variable degrees of heteroplasmy and complex I activity were found in all tissues	Leber optic neuropathy with dystonia, Leigh syndrome	Affected complex I active/deactive state transition, located at a loop crucial for the A/D transition of the enzyme	[10]
		Ile60Thr	N/A		Leber hereditary optic atrophy	Affected assembly due to impaired interaction of ND3, ND4L and ND6 subunits; placed off the proton translocation site with the side chain at the interface with ND4L and ND6 subunits	[114]
		Glu66Asn	<65		Leigh syndrome	Affected assembly due to impaired interaction of ND3, ND1 and ND6 subunits; located at a TMH forming interaction with ND1 and ND6 subunits	[115]
MT-ND2 ND2	Membrane domain/ core	Ile57Met	100	Biochemical analysis of complex I in patient lymphoblasts and transmitochondrial cybrids demonstrated a respiration defect with complex-I-linked substrates, although the specific activity of complex I was not reduced	Leber hereditary optic atrophy	Affected assembly due to impaired interaction of ND2 and ND4L subunits; placed at the interface with ND4L subunit	[116]
		Leu71Pro	51	Accumulation of the membrane arm assembly intermediate 400 kDa and the peripheral arm assembly 600 kDa subcomplexes	Leigh syndrome	TM6 likely distorted. Affected assembly due to impaired interaction with ND4L subunit	[117]
		Gly259Ser	N/A	Resistance to rotenone in humans, 90% activity E. coli	Leber hereditary optic atrophy	Disruption of proton translocation through the ND2 channel; located on the loop in the center of the broken TMH12, close to the key Lys263	[118,119]
MT-ND1 ND1	Membrane domain/ core	Val11Met	<70	co-segregates with tRNALeu(CUN) A12308G and tRNAThr C15946T mutations	Leber hereditary optic atrophy	Disruption of electron transfer by obstruction of Q entry site; located at the first TM helix building entry channel for quinone	[120]
		Glu24Lys	<40		Leber hereditary optic atrophy	Disruption of electron transfer by distortion of Q entry site; located at the first TM helix building entry channel for quinone	[121]
		Leu28Met	40	Decrease in complex I protein level	Deafness	Disruption of electron transfer by distortion of Q entry site; located at the first TM helix building entry channel for quinone	[122]
		Tyr30His	N/A		Leber hereditary optic atrophy	Disruption of electron transfer by distortion of Q entry site; located at the first TM helix building entry channel for quinone	[123]

		Mutation	Activity	Notes	Disease	Mechanism	Ref
		Met31Val	N/A		Alzheimer and Parkinson disease	Disruption of electron transfer by distortion of Q entry site; located at the first TM helix building entry channel for quinone	[124]
		Ala52Thr	<39		Leber hereditary optic atrophy	Disruption of electron transfer by obstruction of Q entry site; located at amphipathic α-helix building entry channel for quinone	[125]
		Met53Ile	N/A		Leber hereditary optic atrophy, Leigh syndrome	Disruption of electron transfer by obstruction of Q entry site; located at amphipathic α-helix building entry channel for quinone	[126]
		Glu59Lys	N/A		Leigh syndrome	Disruption of electron transfer by distortion of Q entry site; located at amphipathic α-helix building entry channel for quinone	[127]
		Ser110Asn	100	Respiration defect with complex I-linked substrates in patient lymphoblasts and trans-mitochondrial cybrids, but specific activity of complex I was not reduced	Leber hereditary optic atrophy	Possible disruption of proton translocation pathway through the E-channel	[116]
		Ala112Thr	N/A		Leber hereditary optic atrophy	Disruption of proton translocation through the E-channel	[109]
		Gly131Ser	40	Complex I activity decreased in fibroblasts but normal in muscles	MELAS, Leber hereditary optic atrophy	Possible distortion of Q-binding cavity; interacts with the key TMH5-6 loop lining the cavity	[128]
		Ala132Thr	N/A		Leber hereditary optic atrophy	Possible distortion of Q-binding cavity; interacts with the key TMH5-6 loop lining the cavity	[129]
		Glu143Lys	N/A		Leber hereditary optic atrophy	Disruption of proton translocation through the E-channel, connects half-channels of the proton translocation unit	[130]
		Ala164Thr	Decreased CI activity		Dystonia	Affected assembly due to misfolding of ND1 subunit; located in the center of a short α-helix stabilizing TMHs 2-6	[131]
		Arg195Gln	<60		Leigh syndrome	Disruption of quinone binding; lines the Q-cavity	[127]
		Val208Leu	<80	Complex I assembly intact	Leigh syndrome	Impairment of coupling, located in the region proposed to link quinone reduction and proton pumping sites	[132]
		Glu214Lys	<63		MELAS	Impairment of coupling, located in the region proposed to link quinone reduction and proton pumping sites	[128]
		Tyr215His	63		MELAS	Impairment of coupling, located in the region proposed to link quinone reduction and proton pumping sites	[128]
		Thr240Met	N/A		Leber hereditary optic atrophy	Affected assembly or destabilization of ND1 subunit, located at the C-terminus of the TMH6	[99]
		Tyr227Cys	14		Leber hereditary optic atrophy	Disruption of electron transfer by distortion of Q entry site; located on TMH6, framing the entry site	[125]
		Leu285Pro	27		Leber hereditary optic atrophy	Affected assembly due to impaired interactions of ND1 with ND3 and NDUFS2 subunits	[125]
		Leu289Met	N/A		Leber hereditary optic atrophy	Affected assembly due to impaired interactions of ND1 with ND3 subunit	[133]
NDUFS4 18kDa	Peripheral domain/ supernumerary	Asp119His (77)	63	Reduction in complex I activity in muscle homogenate but normal activities in cultured fibroblasts	Leigh syndrome	Affected assembly due to impaired interaction of NDUFS4, NDUFA9, NDUFV1 and NDUFS1 subunits; located on a loop anchored in between the neighboring NDUFS3, NDUFV1, NDUFS1 core subunits	[134]
NDUFS6 13kDa	Peripheral domain/ supernumerary	Cys115Tyr (87)	<22		Fatal neonatal lactic acidemia	Affected assembly due to misfolding of 13kDa subunit and disruption of electron transfer at N5 cluster site; one of the amino acids coordinating Zn ion	[135]

Subunit	Domain	Mutation	%	Assembly	Disease	Effect	Ref
NDUFA9 39kDa	Peripheral domain/ supernumerary	Arg321Pro (286)	<30		Leigh syndrome	Affected assembly due to misfolding of NDUFA9 subunit; one of the amino acids coordinating NADPH	[52]
		Arg360Cys (325)	<61	accumulation of several low and high molecular weight complex I assembly intermediates	Miscellaneous: dystonia, dysarthria, Leigh syndrome, raised blood lactate	Affected assembly due to impaired interaction of NDUFA9, NDUFA6 and ND3 subunits; located on a loop making contacts with NDUFA6 and ND3 subunits	[136]
NDUFA1 MWFE	Membrane domain/ supernumerary	Gly8Arg (8)	<20	decreased levels of intact complex I with no accumulation of lower molecular weight subcomplexes.	Encephalomyopathy	Affected assembly due to impaired interaction of NDUFA1 and ND1 subunits	[137]
		Gly32Arg (32)	<50		Encephalomyopathy	Affected assembly due to impaired interaction of NDUFA1, NDUFA8, NDUFA13 and ND1 subunits; located at a loop interacting with NDUFA8, ND1 and NDUFA13	[63,138]
		Arg37Ser (37)	<70	decreased levels of intact complex I with no accumulation of lower molecular weight subcomplexes	Encephalomyopathy	Affected assembly due to impaired interaction of NDUFA1, NDUFA8, NDUFA13 and ND1 subunits; located at a loop interacting with NDUFA8, ND1 and NDUFA13	[137]
NDUFA8 PGIV	Membrane domain/ supernumerary	[a]Glu109Lys (108)	N/A		Miscellaneous: neonatal hypotonia, dysmorphic features, epilepsy and signs of brainstem involvement, lactic acidosis	Change is associated with instability of the mutant transcript	[54]
NDUFA10 42kDa	Membrane domain/ supernumerary	Gly99Glu (64)	<25		Encephalomyopathy	Affected assembly due to misfolding of NDUFA10 subunit, located at the interface with the ND2 and NDUFC1 (KFYI) subunits	[63]
		Gln142Arg (107)	<29		Leigh syndrome	Affected assembly due to misfolding of NDUFA10 subunit	[139]
NDUFA13 B16.6	Membrane domain/ supernumerary	Lys5Asn (4)[d]	N/A		Tumours of thyroid	Affected assembly due to impaired interaction of NDUFA13 and NDUFA7 subunits, located at a start of the N-terminal coil which binds to the NDUFA7 subunit	[140]
NDUFB9 B22	Membrane domain/ supernumerary	Leu64Pro (63)	>50		Miscellaneous: raised blood lactate, muscular hypotonia	Affected assembly due to impaired interaction of NDUFB9 and NDUFAB1 subunits, located at PNS co-factor binding pocket	[63]

[a]in ovine complex I lysine is the natural variant in this position
[b]described as 'P113L'
[c]described as 'D445N'
[d]described as 'K88N'
LHON, Leber's hereditary optic neuropathy; MELAS, childhood-onset mitochondrial encephalomyopathy and lactic acidosis and stroke-like episodes syndrome; PNS, phosphopantetheine; Q, ubiquinone; WB, western blot.

Box 1 Putative mechanism of coupling between electron transfer and proton translocation in mammalian complex I.

The proposed mechanism [15,21] involves long-range conformational changes, allowing for redox energy of electron transfer, released in the peripheral (matrix) arm, to be used to drive proton translocation in the membrane arm. The electron transfer pathway begins with NADH donating two electrons to a flavin mononucleotide (FMN) molecule bound at the tip of the peripheral arm (Figures 1 and I). These electrons are then transferred in turn via a chain of seven iron-sulfur (FeS) clusters to ubiquinone (Q) bound at the interface between the peripheral and membrane arms. Upon electron

transfer, negatively charged quinone (or charged residues nearby) initiate a cascade of conformational changes, indicated by a series of double red arrows (Figure I). Shifts of helices near the cluster N2 may help initiate these changes [141]. They originate around the so-called E-channel, a proton translocation channel formed near the Q-site by subunits ND1, ND3, ND6 and ND4L [15]. Additionally, three antiporter-like subunits (ND2, ND4 and ND5) each contain a single proton channel formed by two connected half-channels, with key Lys/Glu residues sitting on breaks in TM helices (blue/red circles) [15,21]. Black arrows in Figure I indicate possible proton transfer pathways. Conformational changes propagate from the Q site/E-channel to the antiporter-like subunits via the central flexible hydrophilic axis, causing changes both in pKa and in access to proton networks of key Lys/Glu residues. ND5 helix HL and traverse helices from four supernumerary subunits on the IMS side (NDUFB10, NDUFB5, NDUFS5 and NDUFA8) may serve as stators. Subunits NDUFA10 and NDUFA5 provide additional, possibly regulatory, contact between the peripheral and membrane arms. Green and red arrows around the tip of PA indicate the proposed shift of the arm in transition between different states (A/D or catalytic). This movement is correlated with re-organisation (green/red arrows) of the $\beta1$-$\beta2^{NDUFS2(49kDa)}$ and $\alpha1$-$\alpha2^{ND3}$ loops pictured as black lines. The NADPH-containing NDUFA9 (39kDa) subunit [53] and Zn-containing NDUFS6 (13kDa) subunit [51] are essential for activity and may serve as redox sensors. Both NDUFAB1 (SDAP) subunits interact with their LYR partners (NDUFA6 and NDUFB9) via flipped-out phosphopantetheine (black line). The net result of one conformational cycle, driven by NADH:ubiquinone oxidoreduction, is the translocation of four protons across the membrane.

Figure I. Graphical overview of the putative complex I mechanism and associated conformational changes. Core and putatively regulatory or stabilizing supernumerary subunits, discussed in Box 1, are shown.

Figure 1. Architecture of respiratory complex I.

Complex I core subunits, conserved from bacteria, are shown in different colours for each of the modules: N-module (NADH-oxidizing), Q-module (connecting) and the proximal (Pp) and distal (Pd) proton-pumping modules. Approximate position of the membrane is indicated, and the Fe-S clusters and FMN in the matrix arm are shown as spheres. All supernumerary subunits are shown in transparent grey. Illustrated using atomic structure of the mammalian (ovine) complex I (PDB: 5LNK) [21].

Figure 2. Comparison of recently published structures of complex I. Complex I pictured as a cartoon (panels A, C and E) or ribbon (panels B, D and F) and aligned by ND1-ND4 subunits (Box 1). Ovine complex I (PDB: 5LNK) is shown in blue, porcine (PDB: 5GUP) in red and bovine (PDB: 5LC5) in green. Arrows indicate the direction of movement and rotation of the PA and MD. Dashed lines indicate cross-sections shown in corresponding panels. (**A**) Side view of complex I. (**B**) Approximately perpendicular

to the rotation axis cross-section of complex I PA. (**C**) 'Back' view of complex I. (**D**) Cross section of complex I MD approximately in the middle of the inner mitochondrial membrane. (**E**) Matrix side view of complex I. (**F**) Ubiquinone (Q) binding site of complex I with the crucial β1-β2$^{NDUFS2(49kDa)}$ loop and Q molecule modelled based on the *T. thermophilus* structure (PDB: 4HEA). MD, membrane domain; PA, peripheral arm.

Figure 3. Overview of complex I deficiency-causing mutations. Complex I is depicted as a transparent cartoon with core matrix arm subunits coloured in orange, core membrane arm subunits in blue, supernumerary subunits bearing mutations in pink and mutations-free in green. Amino acids mutated in patients suffering from complex I dysfunction are presented as spheres. Leigh syndrome in red, LHON in purple, broad-spectrum phenotype in black and other diseases in yellow. LHON, Leber's hereditary optic neuropathy.

Figure 4. Examples of disease causing-mutations in human complex I. Proteins are pictured as a cartoon with each subunit in a different color, natural variants of amino acids as light pink sticks and disease-causing substitutions as black sticks. Co-factors are labelled in bold. (**A**) NDUFS1 (75kDa) subunit. (**B**) NDUFV1 (51kDa) subunit. (**C**) NDUFS2 (49kDa) subunit. (**D**) NDUFS8 (TYKY) subunit. (**E**) ND1 subunit. (**F**) ND6 subunit. (**G**) NDUFS6 (13kDa) subunit. (**H**) NDUFB9 (B22) subunit in blue and NDUFAB1-β (SDAP-β) subunit in pink. (**I**) ND5 subunit. (**J**) NDUFA9 (39kDa) subunit. (**K**) NDUFA1 (MWFE) subunit. (**L**) NDUFA10 (42kDa) subunit.

References

1. Moser, C.C., *et al.* (2006) Electron tunneling chains of mitochondria. *Biochim. Biophys. Acta* 1757, 1096-1109

2. Walker, J.E. (2013) The ATP synthase: the understood, the uncertain and the unknown. *Biochem Soc Trans* 41, 1-16

3. Kirby, D.M., *et al.* (1999) Respiratory chain complex I deficiency: an underdiagnosed energy generation disorder. *Neurology* 52, 1255-1264

4. Koene, S., *et al.* (2012) Natural disease course and genotype-phenotype correlations in Complex I deficiency caused by nuclear gene defects: what we learned from 130 cases. *J Inherit Metab Dis* 35, 737-747

5. Fassone, E. and Rahman, S. (2012) Complex I deficiency: clinical features, biochemistry and molecular genetics. *J Med Genet* 49, 578-590

6. Tucker, E.J., *et al.* (2011) The molecular basis of human complex I deficiency. *IUBMB Life* 63, 669-677

7. Wallace, D.C., *et al.* (1988) Mitochondrial DNA mutation associated with Leber's hereditary optic neuropathy. *Science* 242, 1427-1430

8. Deschauer, M., *et al.* (2003) Late-onset encephalopathy associated with a C11777A mutation of mitochondrial DNA. *Neurology* 60, 1357-1359

9. Tuppen, H.A., *et al.* (2010) The p.M292T NDUFS2 mutation causes complex I-deficient Leigh syndrome in multiple families. *Brain* 133, 2952-2963

10. Sarzi, E., *et al.* (2007) A novel recurrent mitochondrial DNA mutation in ND3 gene is associated with isolated complex I deficiency causing Leigh syndrome and dystonia. *Am J Med Genet A* 143a, 33-41

11. Formosa, L.E., *et al.* (2018) Building a complex complex: Assembly of mitochondrial respiratory chain complex I. *Semin Cell Dev Biol* 76, 154-162

12. Guerrero-Castillo, S., *et al.* (2017) The Assembly Pathway of Mitochondrial Respiratory Chain Complex I. *Cell Metab* 25, 128-139

13. Sazanov, L.A. and Hinchliffe, P. (2006) Structure of the hydrophilic domain of respiratory complex I from Thermus thermophilus. *Science* 311, 1430-1436

14. Efremov, R.G. and Sazanov, L.A. (2011) Structure of the membrane domain of respiratory complex I. *Nature* 476, 414-420

15. Baradaran, R., *et al.* (2013) Crystal structure of the entire respiratory complex I. *Nature* 494, 443-448

16. Jones, A.J., *et al.* (2017) Respiratory Complex I in Bos taurus and Paracoccus denitrificans Pumps Four Protons across the Membrane for Every NADH Oxidized. *J Biol Chem* 292, 4987-4995

17. Walker, J.E. (1992) The NADH - ubiquinone oxidoreductase (complex I) of respiratory chains. *Q. Rev. Biophys.* 25, 253-324

18. Brandt, U. (2006) Energy converting NADH:quinone oxidoreductase (complex I). *Annu. Rev. Biochem.* 75, 69-92

19. Zickermann, V., *et al.* (2015) Structural biology. Mechanistic insight from the crystal structure of mitochondrial complex I. *Science* 347, 44-49

20. Zhu, J., *et al.* (2016) Structure of mammalian respiratory complex I. *Nature* 536, 354-358

21. Fiedorczuk, K., *et al.* (2016) Atomic structure of the entire mammalian mitochondrial complex I. *Nature* 538, 406-410

22. Wu, M., *et al.* (2016) Structure of Mammalian Respiratory Supercomplex I1III2IV1. *Cell* 167, 1598-1609 e1510

23. Guo, R*., et al.* (2017) Architecture of Human Mitochondrial Respiratory Megacomplex I2III2IV2. *Cell* 170, 1247-1257 e1212

24. Letts, J.A*., et al.* (2016) Purification of Ovine Respiratory Complex I Results in a Highly Active and Stable Preparation. *J Biol Chem*

25. Enriquez, J.A. (2016) Supramolecular Organization of Respiratory Complexes. *Annu Rev Physiol* 78, 533-561

26. Letts, J.A*., et al.* (2016) The architecture of respiratory supercomplexes. *Nature* 537, 644-648

27. Gu, J*., et al.* (2016) The architecture of the mammalian respirasome. *Nature* 537, 639-643

28. Biasini, M*., et al.* (2014) SWISS-MODEL: modelling protein tertiary and quaternary structure using evolutionary information. *Nucleic Acids Res* 42, W252-258

29. Adams, P.D*., et al.* (2010) PHENIX: a comprehensive Python-based system for macromolecular structure solution. *Acta Crystallogr D Biol Crystallogr* 66, 213-221

30. Galkin, A*., et al.* (2008) Identification of the mitochondrial ND3 subunit as a structural component involved in the active/deactive enzyme transition of respiratory complex I. *J. Biol. Chem.* 283, 20907-20913

31. Kotlyar, A.B. and Vinogradov, A.D. (1990) Slow active/inactive transition of the mitochondrial NADH-ubiquinone reductase. *Biochim Biophys Acta* 1019, 151-158

32. Maklashina, E*., et al.* (2003) Active/de-active transition of respiratory complex I in bacteria, fungi, and animals. *Biochim Biophys Acta* 1606, 95-103

33. Ciano, M*., et al.* (2013) Conformation-specific crosslinking of mitochondrial complex I. *FEBS Lett* 587, 867-872

34. Roberts, P.G. and Hirst, J. (2012) The deactive form of respiratory complex I from mammalian mitochondria is a Na+/H+ antiporter. *J Biol Chem* 287, 34743-34751

35. Verkhovskaya, M. and Bloch, D.A. (2013) Energy-converting respiratory Complex I: on the way to the molecular mechanism of the proton pump. *Int J Biochem Cell Biol* 45, 491-511

36. Rodenburg, R.J. (2016) Mitochondrial complex I-linked disease. *Biochim Biophys Acta* 1857, 938-945

37. Stroud, D.A*., et al.* (2016) Accessory subunits are integral for assembly and function of human mitochondrial complex I. *Nature* 538, 123-126

38. Rhein, V.F*., et al.* (2016) NDUFAF5 Hydroxylates NDUFS7 at an Early Stage in the Assembly of Human Complex I. *J Biol Chem* 291, 14851-14860

39. Rhein, V.F*., et al.* (2013) NDUFAF7 methylates arginine 85 in the NDUFS2 subunit of human complex I. *J Biol Chem* 288, 33016-33026

40. Andrews, B*., et al.* (2013) Assembly factors for the membrane arm of human complex I. *Proc Natl Acad Sci U S A* 110, 18934-18939

41. Sazanov, L.A. (2007) Respiratory complex I: mechanistic and structural insights provided by the crystal structure of the hydrophilic domain. *Biochemistry* 46, 2275-2288

42. Sato, M*., et al.* (2014) Essential regions in the membrane domain of bacterial complex I (NDH-1): the machinery for proton translocation. *J Bioenerg Biomembr* 46, 279-287

43. Wirth, C*., et al.* (2016) Structure and function of mitochondrial complex I. *Biochim Biophys Acta* 1857, 902-914
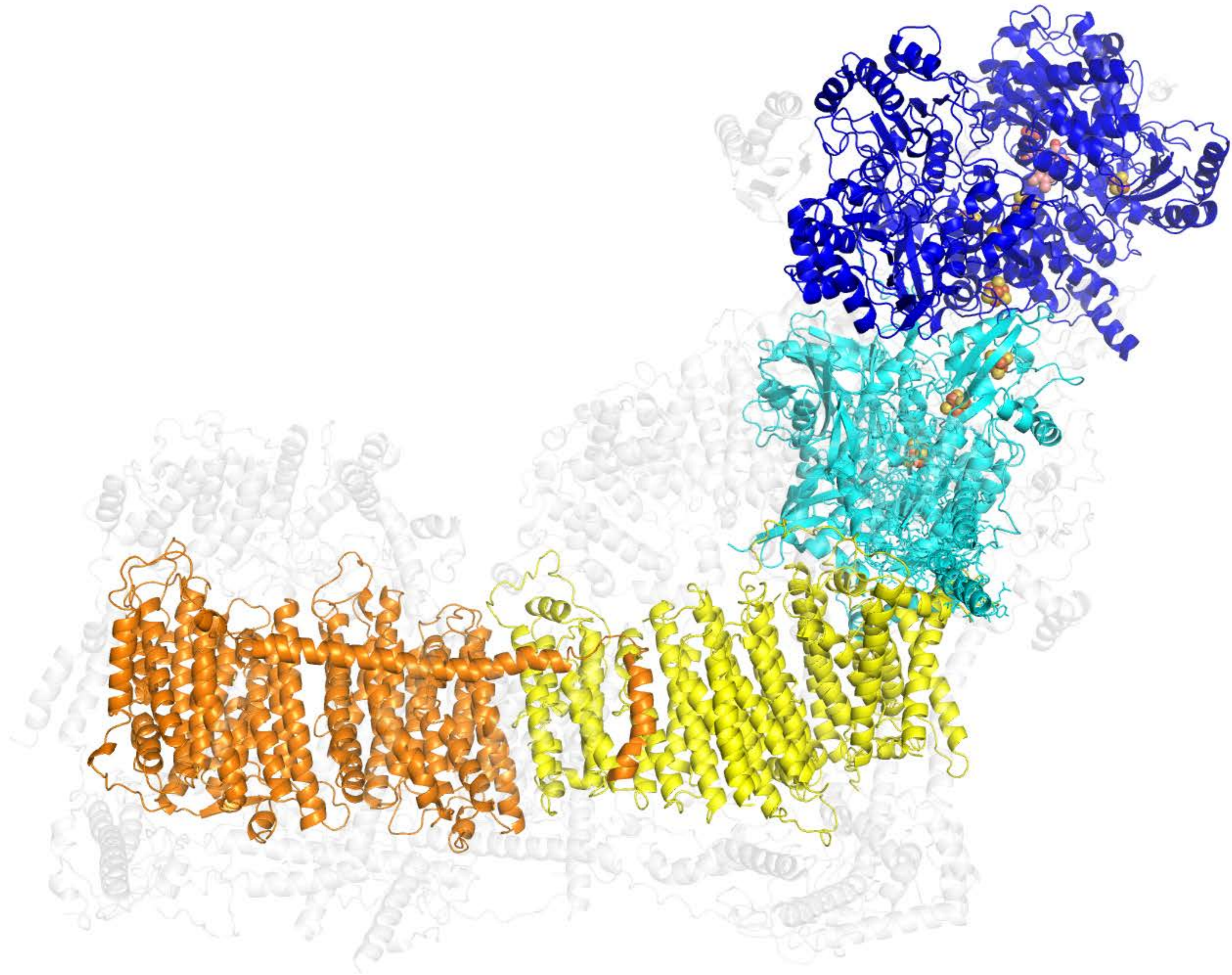
44. Angerer, H., *et al.* (2012) Tracing the tail of ubiquinone in mitochondrial complex I. *Biochimica et biophysica acta*

45. Friedrich, T. (2014) On the mechanism of respiratory complex I. *J Bioenerg Biomembr* 46, 255-268

46. Hirst, J. and Roessler, M.M. (2015) Energy conversion, redox catalysis and generation of reactive oxygen species by respiratory complex I. *Biochim Biophys Acta* 1857, 872-883

47. Grgic, L., *et al.* (2004) Functional significance of conserved histidines and arginines in the 49-kDa subunit of mitochondrial complex I. *J. Biol. Chem.* 279, 21193-21199

48. Zwicker, K., *et al.* (2006) The Redox-Bohr group associated with iron-sulfur cluster N2 of complex I. *J. Biol. Chem.* 281, 23013-23017

49. Friedrich, T. and Scheide, D. (2000) The respiratory complex I of bacteria, archaea and eukarya and its module common with membrane-bound multisubunit hydrogenases. *FEBS Lett.* 479, 1-5

50. Babot, M. and Galkin, A. (2013) Molecular mechanism and physiological role of active-deactive transition of mitochondrial complex I. *Biochem Soc Trans* 41, 1325-1330

51. Kmita, K., *et al.* (2015) Accessory NUMM (NDUFS6) subunit harbors a Zn-binding site and is essential for biogenesis of mitochondrial complex I. *Proceedings of the National Academy of Sciences of the United States of America* 112, 5685-5690

52. van den Bosch, B.J., *et al.* (2012) Defective NDUFA9 as a novel cause of neonatally fatal complex I disease. *J Med Genet* 49, 10-15

53. Abdrakhmanova, A., *et al.* (2006) Tight binding of NADPH to the 39-kDa subunit of complex I is not required for catalytic activity but stabilizes the multiprotein complex. *Biochim Biophys Acta* 1757, 1676-1682

54. Bugiani, M., *et al.* (2004) Clinical and molecular findings in children with complex I deficiency. *Biochim Biophys Acta* 1659, 136-147

55. Parikh, S., *et al.* (2009) A modern approach to the treatment of mitochondrial disease. *Curr Treat Options Neurol* 11, 414-430

56. Anderson, A.C. (2003) The process of structure-based drug design. *Chem Biol* 10, 787-797

57. Vinothkumar, K.R. and Henderson, R. (2016) Single particle electron cryomicroscopy: trends, issues and future perspective. *Q Rev Biophys* 49, e13

58. Kuhlbrandt, W. (2015) Structure and function of mitochondrial membrane protein complexes. *BMC Biol* 13, 89

59. Davies, K.M., *et al.* (2018) Conserved in situ arrangement of complex I and III2 in mitochondrial respiratory chain supercomplexes of mammals, yeast, and plants. *Proc Natl Acad Sci U S A* 115, 3024-3029

60. Haack, T.B., *et al.* (2012) Mutation screening of 75 candidate genes in 152 complex I deficiency cases identifies pathogenic variants in 16 genes including NDUFB9. *J Med Genet* 49, 83-89

61. Danhauser, K., *et al.* (2011) Cellular rescue-assay aids verification of causative DNA-variants in mitochondrial complex I deficiency. *Mol Genet Metab* 103, 161-166

62. Pagniez-Mammeri, H., *et al.* (2009) Rapid screening for nuclear genes mutations in isolated respiratory chain complex I defects. *Mol Genet Metab* 96, 196-200
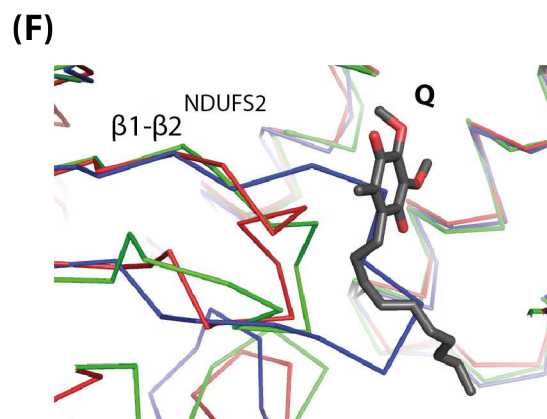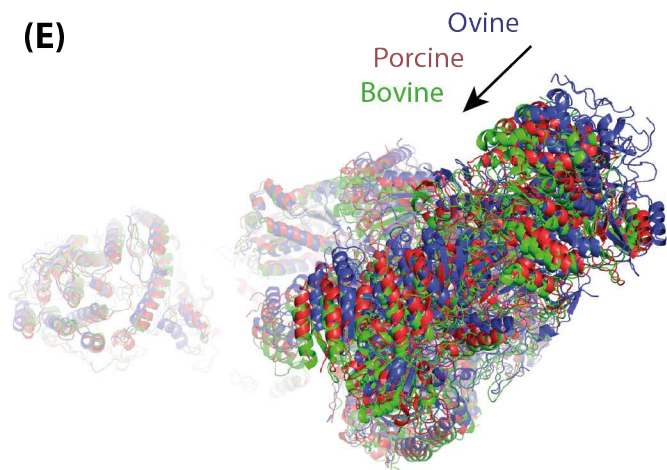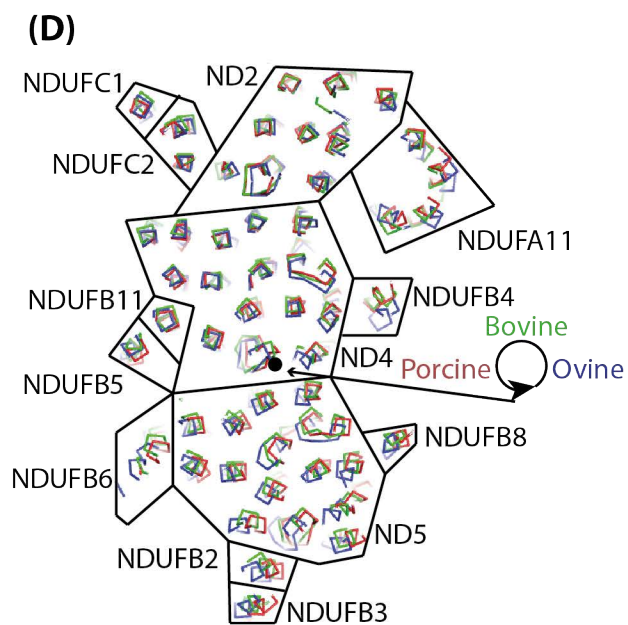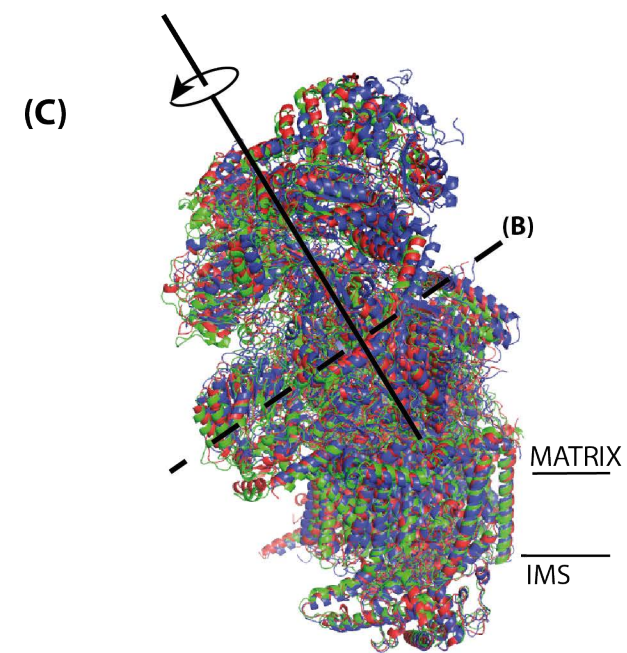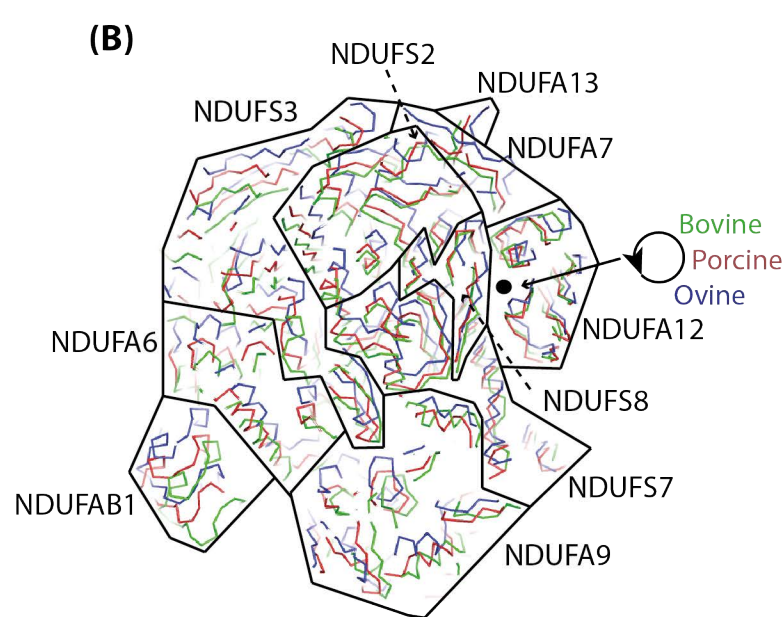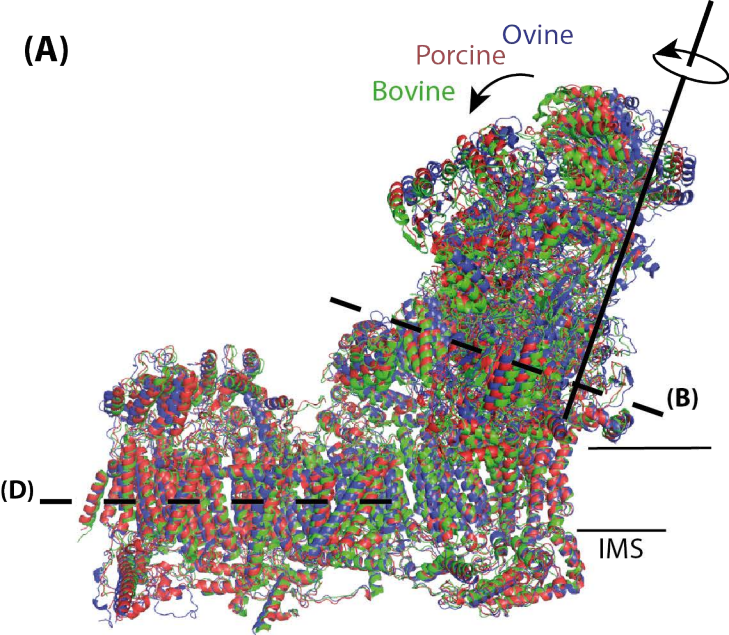
63. Haack, T.B.*, et al.* (2012) Molecular diagnosis in mitochondrial complex I deficiency using exome sequencing. *J Med Genet* 49, 277-283

64. Hoefs, S.J.*, et al.* (2010) Novel mutations in the NDUFS1 gene cause low residual activities in human complex I deficiencies. *Mol Genet Metab* 100, 251-256

65. Martin, M.A.*, et al.* (2005) Leigh syndrome associated with mitochondrial complex I deficiency due to a novel mutation in the NDUFS1 gene. *Arch. Neurol.* 62, 659-661

66. Benit, P.*, et al.* (2001) Large-scale deletion and point mutations of the nuclear NDUFV1 and NDUFS1 genes in mitochondrial complex I deficiency. *Am. J. Hum. Genet.* 68, 1344-1352

67. Ferreira, M.*, et al.* (2011) Progressive cavitating leukoencephalopathy associated with respiratory chain complex I deficiency and a novel mutation in NDUFS1. *Neurogenetics* 12, 9-17

68. Visch, H.J.*, et al.* (2004) Inhibition of mitochondrial Na+-Ca2+ exchange restores agonist-induced ATP production and Ca2+ handling in human complex I deficiency. *J Biol Chem* 279, 40328-40336

69. Marin, S.E.*, et al.* (2013) Leigh syndrome associated with mitochondrial complex I deficiency due to novel mutations In NDUFV1 and NDUFS2. *Gene* 516, 162-167

70. Lieber, D.S.*, et al.* (2013) Targeted exome sequencing of suspected mitochondrial disorders. *Neurology* 80, 1762-1770

71. Schuelke, M.*, et al.* (2002) New nuclear encoded mitochondrial mutation illustrates pitfalls in prenatal diagnosis by biochemical methods. *Clin Chem* 48, 772-775

72. Schuelke, M.*, et al.* (1999) Mutant NDUFV1 subunit of mitochondrial complex I causes leukodystrophy and myoclonic epilepsy. *Nat Genet* 21, 260-261

73. Breningstall, G.N.*, et al.* (2008) Siblings with leukoencephalopathy. *Semin Pediatr Neurol* 15, 212-215

74. Loeffen, J.*, et al.* (2001) Mutations in the complex I NDUFS2 gene of patients with cardiomyopathy and encephalomyopathy. *Ann Neurol* 49, 195-201

75. McFarland, R.*, et al.* (2009) Recurrent mutations in the NDUFS2 gene causing isolated complex I deficiency in skeletal muscle. *Neuromuscular Disorders* 19, 562-562

76. Distelmaier, F.*, et al.* (2009) Mitochondrial complex I deficiency: from organelle dysfunction to clinical disease. *Brain* 132, 833-842

77. Benit, P.*, et al.* (2004) Mutant NDUFS3 subunit of mitochondrial complex I causes Leigh syndrome. *J Med Genet* 41, 14-17

78. Nishioka, K.*, et al.* (2010) Genetic variation of the mitochondrial complex I subunit NDUFV2 and Parkinson's disease. *Parkinsonism Relat Disord* 16, 686-687

79. Marina, A.D.*, et al.* (2013) NDUFS8-related Complex I Deficiency Extends Phenotype from "PEO Plus" to Leigh Syndrome. *JIMD Rep* 10, 17-22

80. Loeffen, J.*, et al.* (1998) The first nuclear-encoded complex I mutation in a patient with Leigh syndrome. *Am J Hum Genet* 63, 1598-1608

81. Procaccio, V. and Wallace, D.C. (2004) Late-onset Leigh syndrome in a patient with mitochondrial complex I NDUFS8 mutations. *Neurology* 62, 1899-1901

82. Visch, H.J.*, et al.* (2006) Decreased agonist-stimulated mitochondrial ATP production caused by a pathological reduction in endoplasmic reticulum calcium content in human complex I deficiency. *Biochim Biophys Acta* 1762, 115-123

83. Triepels, R.H., *et al.* (1999) Leigh syndrome associated with a mutation in the NDUFS7 (PSST) nuclear encoded subunit of complex I. *Ann Neurol* 45, 787-790

84. Lebon, S., *et al.* (2007) A novel mutation in the human complex I NDUFS7 subunit associated with Leigh syndrome. *Mol Genet Metab* 90, 379-382

85. Yu-Wai-Man, P. and Chinnery, P.F. (1993) Leber Hereditary Optic Neuropathy. In *GeneReviews(R)* (Pagon, R.A., *et al.*, eds), University of Washington, Seattle.

86. Wissinger, B., *et al.* (1997) Mutation analysis of the ND6 gene in patients with Lebers hereditary optic neuropathy. *Biochem Biophys Res Commun* 234, 511-515

87. Chinnery, P.F., *et al.* (2001) The mitochondrial ND6 gene is a hot spot for mutations that cause Leber's hereditary optic neuropathy. *Brain* 124, 209-218

88. Macmillan, C., *et al.* (2000) Predominance of the T14484C mutation in French-Canadian families with Leber hereditary optic neuropathy is due to a founder effect. *Am J Hum Genet* 66, 332-335

89. Carelli, V., *et al.* (1999) Biochemical features of mtDNA 14484 (ND6/M64V) point mutation associated with Leber's hereditary optic neuropathy. *Ann Neurol* 45, 320-328

90. Valentino, M.L., *et al.* (2002) Mitochondrial DNA nucleotide changes C14482G and C14482A in the ND6 gene are pathogenic for Leber's hereditary optic neuropathy. *Ann Neurol* 51, 774-778

91. Kirby, D.M., *et al.* (2000) Leigh disease caused by the mitochondrial DNA G14459A mutation in unrelated families. *Ann Neurol* 48, 102-104

92. Shoffner, J.M., *et al.* (1995) Leber's hereditary optic neuropathy plus dystonia is caused by a mitochondrial DNA point mutation. *Ann Neurol* 38, 163-169

93. Ravn, K., *et al.* (2001) An mtDNA mutation, 14453G-->A, in the NADH dehydrogenase subunit 6 associated with severe MELAS syndrome. *Eur J Hum Genet* 9, 805-809

94. Jun, A.S., *et al.* (1994) A mitochondrial DNA mutation at nucleotide pair 14459 of the NADH dehydrogenase subunit 6 gene associated with maternally inherited Leber hereditary optic neuropathy and dystonia. *Proc Natl Acad Sci U S A* 91, 6206-6210

95. Howell, N., *et al.* (2003) Sequence analysis of the mitochondrial genomes from Dutch pedigrees with Leber hereditary optic neuropathy. *Am J Hum Genet* 72, 1460-1469

96. Zhadanov, S.I., *et al.* (2005) A novel mtDNA ND6 gene mutation associated with LHON in a Caucasian family. *Biochem Biophys Res Commun* 332, 1115-1121

97. Taylor, R.W., *et al.* (2002) Leigh disease associated with a novel mitochondrial DNA ND5 mutation. *Eur J Hum Genet* 10, 141-144

98. Liolitsa, D., *et al.* (2003) Is the mitochondrial complex I ND5 gene a hot-spot for MELAS causing mutations? *Ann Neurol* 53, 128-132

99. Huoponen, K., *et al.* (1993) The spectrum of mitochondrial DNA mutations in families with Leber hereditary optic neuroretinopathy. *Hum Genet* 92, 379-384

100. Mayorov, V., *et al.* (2005) The role of the ND5 gene in LHON: characterization of a new, heteroplasmic LHON mutation. *Ann Neurol* 58, 807-811

101. Naini, A.B., *et al.* (2005) Novel mitochondrial DNA ND5 mutation in a patient with clinical features of MELAS and MERRF. *Arch Neurol* 62, 473-476

102. Crimi, M., *et al.* (2003) A missense mutation in the mitochondrial ND5 gene associated with a Leigh-MELAS overlap syndrome. *Neurology* 60, 1857-1861

103. Sudo, A., *et al.* (2004) Leigh syndrome caused by mitochondrial DNA G13513A mutation: frequency and clinical features in Japan. *J Hum Genet* 49, 92-96

104. Aitullina, A., *et al.* (2013) Point mutations associated with Leber hereditary optic neuropathy in a Latvian population. *Mol Vis* 19, 2343-2351

105. Howell, N., *et al.* (1993) When does bilateral optic atrophy become Leber hereditary optic neuropathy? *Am J Hum Genet* 53, 959-963

106. Polyak, K., *et al.* (1998) Somatic mutations of the mitochondrial genome in human colorectal tumours. *Nat Genet* 20, 291-293

107. Brown, M.D., *et al.* (2002) The role of mtDNA background in disease expression: a new primary LHON mutation associated with Western Eurasian haplogroup J. *Hum Genet* 110, 130-138

108. Leo-Kottler, B., *et al.* (2002) Leber's hereditary optic neuropathy: clinical and molecular genetic results in a patient with a point mutation at np T11253C (isoleucine to threonine) in the ND4 gene and spontaneous recovery. *Graefes Arch Clin Exp Ophthalmol* 240, 758-764

109. Wang, Q., *et al.* (2005) Clinical and molecular characterization of a Chinese patient with auditory neuropathy associated with mitochondrial 12S rRNA T1095C mutation. *Am J Med Genet A* 133a, 27-30

110. Torres-Bacete, J., *et al.* (2007) Characterization of the NuoM (ND4) subunit in *Escherichia coli* NDH-1: conserved charged residues essential for energy-coupled activities. *J. Biol. Chem.* 282, 36914-36922

111. Komaki, H., *et al.* (2003) A novel mtDNA C11777A mutation in Leigh syndrome. *Mitochondrion* 2, 293-304

112. Vanniarajan, A., *et al.* (2006) Novel mitochondrial mutation in the ND4 gene associated with Leigh syndrome. *Acta Neurol Scand* 114, 350-353

113. McFarland, R., *et al.* (2004) De novo mutations in the mitochondrial ND3 gene as a cause of infantile mitochondrial encephalopathy and complex I deficiency. *Ann Neurol* 55, 58-64

114. Horvath, J., *et al.* (2002) Sequence analysis of Hungarian LHON patients not carrying the common primary mutations. *J Inherit Metab Dis* 25, 323-324

115. Leshinsky-Silver, E., *et al.* (2010) Leigh disease presenting in utero due to a novel missense mutation in the mitochondrial DNA-ND3. *Mol Genet Metab* 100, 65-70

116. Brown, M.D., *et al.* (2001) Novel mtDNA mutations and oxidative phosphorylation dysfunction in Russian LHON families. *Hum Genet* 109, 33-39

117. Hinttala, R., *et al.* (2006) Analysis of mitochondrial DNA sequences in patients with isolated or combined oxidative phosphorylation system deficiency. *J Med Genet* 43, 881-886

118. Brown, M.D., *et al.* (1992) Mitochondrial DNA complex I and III mutations associated with Leber's hereditary optic neuropathy. *Genetics* 130, 163-173

119. Carelli, V., *et al.* (1997) Leber's hereditary optic neuropathy: biochemical effect of 11778/ND4 and 3460/ND1 mutations and correlation with the mitochondrial genotype. *Neurology* 48, 1623-1632

120. Zifa, E., *et al.* (2008) A novel G3337A mitochondrial ND1 mutation related to cardiomyopathy co-segregates with tRNALeu(CUN) A12308G and tRNAThr C15946T mutations. *Mitochondrion* 8, 229-236

121. Blakely, E.L., *et al.* (2005) LHON/MELAS overlap syndrome associated with a mitochondrial MTND1 gene mutation. *Eur J Hum Genet* 13, 623-627

122. Gutierrez Cortes, N., *et al.* (2012) Novel mitochondrial DNA mutations responsible for maternally inherited nonsyndromic hearing loss. *Hum Mutat* 33, 681-689

123. Obayashi, T.*, et al.* (1992) Point mutations in mitochondrial DNA in patients with hypertrophic cardiomyopathy. *Am Heart J* 124, 1263-1269

124. Hutchin, T. and Cortopassi, G. (1995) A mitochondrial DNA clone is associated with increased risk for Alzheimer disease. *Proc Natl Acad Sci U S A* 92, 6892-6895

125. Howell, N.*, et al.* (1991) Leber hereditary optic neuropathy: identification of the same mitochondrial ND1 mutation in six pedigrees. *Am J Hum Genet* 49, 939-950

126. Funalot, B.*, et al.* (2002) Leigh-like encephalopathy complicating Leber's hereditary optic neuropathy. *Ann Neurol* 52, 374-377

127. Moslemi, A.R.*, et al.* (2008) Progressive encephalopathy and complex I deficiency associated with mutations in MTND1. *Neuropediatrics* 39, 24-28

128. Kirby, D.M.*, et al.* (2004) Mutations of the mitochondrial ND1 gene as a cause of MELAS. *J Med Genet* 41, 784-789

129. Fauser, S.*, et al.* (2002) Sequence analysis of the complete mitochondrial genome in patients with Leber's hereditary optic neuropathy lacking the three most common pathogenic DNA mutations. *Biochem Biophys Res Commun* 295, 342-347

130. Valentino, M.L.*, et al.* (2004) The ND1 gene of complex I is a mutational hot spot for Leber's hereditary optic neuropathy. *Ann Neurol* 56, 631-641

131. Simon, D.K.*, et al.* (2003) A heteroplasmic mitochondrial complex I gene mutation in adult-onset dystonia. *Neurogenetics* 4, 199-205

132. Wray, C.D.*, et al.* (2013) A new mutation in MT-ND1 m.3928G>C p.V208L causes Leigh disease with infantile spasms. *Mitochondrion* 13, 656-661

133. Kim, J.Y.*, et al.* (2002) Mitochondrial DNA C4171A/ND1 is a novel primary causative mutation of Leber's hereditary optic neuropathy with a good prognosis. *Ann Neurol* 51, 630-634

134. Leshinsky-Silver, E.*, et al.* (2009) NDUFS4 mutations cause Leigh syndrome with predominant brainstem involvement. *Mol Genet Metab* 97, 185-189

135. Spiegel, R.*, et al.* (2009) Mutated NDUFS6 is the cause of fatal neonatal lactic acidemia in Caucasus Jews. *Eur J Hum Genet* 17, 1200-1203

136. Baertling, F.*, et al.* (2017) NDUFA9 point mutations cause a variable mitochondrial complex I assembly defect. *Clin Genet* 93, 111-118

137. Fernandez-Moreira, D.*, et al.* (2007) X-linked NDUFA1 gene mutations associated with mitochondrial encephalomyopathy. *Ann Neurol* 61, 73-83

138. Potluri, P.*, et al.* (2009) A novel NDUFA1 mutation leads to a progressive mitochondrial complex I-specific neurodegenerative disease. *Mol Genet Metab* 96, 189-195

139. Hoefs, S.J.*, et al.* (2011) NDUFA10 mutations cause complex I deficiency in a patient with Leigh disease. *Eur J Hum Genet* 19, 270-274

140. Maximo, V.*, et al.* (2005) Somatic and germline mutation in GRIM-19, a dual function gene involved in mitochondrial metabolism and cell death, is linked to mitochondrion-rich (Hurthle cell) tumours of the thyroid. *Br J Cancer* 92, 1892-1898

141. Berrisford, J.M. and Sazanov, L.A. (2009) Structural basis for the mechanism of respiratory complex I. *J. Biol. Chem.* 284, 29773-29783

(A) Ovine, Porcine, Bovine

(B) NDUFS3, NDUFS2, NDUFA13, NDUFA7, Bovine, Porcine, Ovine, NDUFA6, NDUFA12, NDUFS8, NDUFS7, NDUFAB1, NDUFA9, IMS

(C) MATRIX, IMS

(D) NDUFC1, ND2, NDUFC2, NDUFA11, NDUFB11, NDUFB4, Bovine, NDUFB5, ND4, Porcine, Ovine, NDUFB6, NDUFB8, NDUFB2, ND5, NDUFB3

(E) Ovine, Porcine, Bovine

(F) β1-β2, NDUFS2, Q